Materials Transactions, Vol. 53, No. 2 (2012) pp. 395 to 400

Dynamic Mechanical Behaviour of Polymer Bonded Nd–Fe–B Composite Materials

Aleksandar Grujić[1,*], Mirko Stijepović[2,3], Jasna Stajić-Trošić[1], Slaviša Putić[2], Dragutin Nedeljković[1], Aleksandar Stajčić[1] and Radoslav Aleksić[2]

[1]*Institute of Chemistry, Technology and Metallurgy, University of Belgrade, Njegoševa 12, 11000 Belgrade, Serbia*
[2]*Faculty of Technology and Metallurgy, University of Belgrade, Karnegijeva 4, 11000 Belgrade, Serbia*
[3]*Department of Chemical Engineering, Texas A&M University at Qatar, Education City P. O. Box 23874, Doha, Qatar*

Magnetic composite materials with varied content of Nd–Fe–B particles in epoxy matrix are examined from a dynamic mechanical perspective. Structural, viscoelastic and magnetic properties of composites have been observed using Scanning Electron Microscope (SEM), Dynamic Mechanical Analysis (DMA) and Super Quantum Interference Device (SQUID) magnetometer, respectively. Experimental results show that magnetic properties and corresponding dynamic mechanical behaviour depend on packing density. Also, results observed by predictive mathematical models suggest that maximal packing factor has a direct impact on elastic behaviour of composites.
[doi:10.2320/matertrans.M2011218]

(Received July 19, 2011; Accepted October 31, 2011; Published January 25, 2012)

Keywords: *neodymium–iron–boron, composite materials, dynamic mechanical analysis (DMA), super quantum interference device (SQUID), epoxy resin*

1. Introduction

Polymer bonded Nd–Fe–B magnetic materials have a very important role as functional components within the wider spectra of contemporary devices in different industrial and consumer sectors.[1–8)] Advantages of the using bonded composite materials include their simple technology, possibility of forming their final properties, low manufacturing costs because of no costly finishing and lowering of material losses resulting from the possibility of forming any shape.[7)]

The amount of Nd–Fe–B powder in the bonded magnet plays a crucial role in determining magnetic properties. A higher content of Nd–Fe–B powder usually results in a higher remanence magnetization (B_r) and maximum energy product $(BH)_{max}$. Therefore, it is desirable from the magnetic perspectives. However, a higher content of magnetic filler may change the rheology of polymer melt during the process, and subsequently, impact the mechanical strength of bonded magnets. Nevertheless, the balance between magnetic properties and corresponding dynamic mechanical behaviour is an important issue for bonded magnet applications.[8)] The advantage of DMA technique compared to the standard mechanical test methods is demonstrated. Predictive mathematical models are employed to evaluate dynamic mechanical behaviour of composites. Results obtained with the proposed mathematical models are in good agreement with experimental values.

2. Experimental

The rapid quenched magnetic powder with a particle size between 74 and 177 µm is used for composites preparation The magnetic properties of the Nd–(Fe,Co)–B were: $B_r = 0.82$ T, $H_{cb} = 477.5$ kA/m, $H_{cj} = 692.3$ kA/m, $(BH)_{max} = 104.2$ kJ/m^3. The chemical composition of the starting magnet alloy is Nd: 21–25 mass%, Co: 3–5 mass%, B <1.5 mass%, Zr: 3–5 mass%, Fe: balance. The thermosetting epoxy system that is a combination of liquid mixture of Bisphenol A and Bisphenol F resins and cross linking agent (hardener) which cures fully at room temperature is used as a polymer matrix. The cured pure epoxy resin has tensile strength ~ 58 MPa, elongation ~ 2.8%, compression strength ~ 96 MPa, flexural strength ~ 78 MPa and density ~ 1.2 g/cm^3.

Composites with varied Nd–Fe–B particle content in the epoxy matrix from 15 to 95 mass% are produced by compression moulding under a pressure of 4 MPa at room temperature, using a lab scale compression moulding press. The production process is carried out under conditions that avoid air bubbles in the mixture. No external magnetic field is used during the cure.

The structure and morphology of Nd–Fe–B powder and fracture surfaces of composites incurred during the tensile tests are observed by JEOL JSM-5800 Scanning Electron Microscope (SEM), with an accelerating voltage of 20 kV. After tensile tests at room temperature, fracture sample surfaces are sputtered with gold using a POLARON SC 502 sputter coater for enhanced conductivity. A TA Instruments DMA Q800 is used to obtain dynamic mechanical data for investigated magnetic composites and pure epoxy samples. These samples are tested using a three-point bend clamp with a 20 mm span width and rectangular-edge probe, at a frequency of 1 Hz. Testing is done over a temperature range from 25 to 100°C with a temperature ramp of 3°C/min. Tensile and flexural tests are performed under ambient temperature conditions using Schenck TREBEL RM100, a universal material testing machine. The macroscopic magnetic properties were determined using Superconducting Quantum Interference Device (SQUID) magnetometer. During ambient temperature (300 K) measurements, the magnetic field strength $\mu_o H$ is varied from −5 to 5 T. Sample preparation and experimental procedures have been conditioned such that the demagnetization factor can be neglected. While the SQUID magnetometer is a very sensitive device,

*Corresponding author, E-mail: gruja@tmf.bg.ac.rs

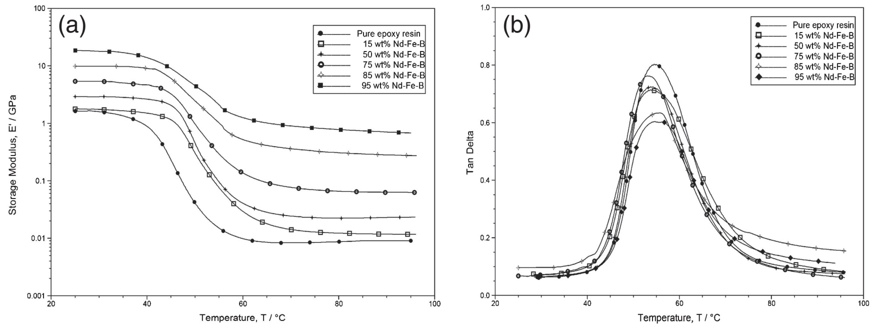

Fig. 1 DMA curves of (a) storage modulus E' and (b) Tan δ, for the pure epoxy resin and the composites with different Nd–Fe–B filler content versus temperature.

a magnetic moment from 10^{-11} up to $10^{3}\,\mathrm{Am}^{2}$ can be measured with an accuracy of 0.1%.

3. Results and Discussion

3.1 Dynamic mechanical properties

Due to the viscoelastic nature of polymer composites, their dynamic and thermal behaviours significantly depend on strain, frequency and temperature. When comparing material properties, a material with a higher storage modulus (E') would be stiffer and harder to deform than one with a lower E'. Besides the elastic component, a material also has a viscous component called the loss modulus (E''). This viscous component relates to the materials ability to lose energy. The material's $\tan\delta$ designates the material's ratio of viscous to elastic components (E''/E') and it is sometimes called the materials damping ability.[9,10] The dynamic mechanical properties of the pure epoxy polymer and the Nd–Fe–B/epoxy magnetic composite materials are studied as a function of temperature, from the glassy to the rubbery state, as reported elsewhere.[11,12] The results presented in Fig. 1(a) show a considerable improvement in the storage modulus (elastic component) caused by the presence of the Nd–Fe–B magnetic filler.

In the glassy region (around 25°C), the total dynamic modulus of composites is directly influenced by the modulus of the pure polymer, modulus of the filler, the concentrations of both, as well as the adhesion factor between the filler and polymer.[13,14] At the other end of temperature range, the storage modulus decreases with the temperature to the lower values in the rubbery state.[15]

DMA results presented in Fig. 1(b) show that a composite material with a higher $\tan\delta$ (≈ 0.7 for composite with 15 mass% of Nd–Fe–B filler) has a higher viscous percentage than one with a lower $\tan\delta$ (≈ 0.6 for composite with 95 mass% of Nd–Fe–B filler). Therefore the material would be more likely to absorb a vibration or impact, and disperse it throughout the material without failure. Glass transition temperatures (T_g) obtained from $\tan\delta$ curves (peak point temperatures) were found within the same temperature region (around 54°C). This could be a consequence of the use of Nd–Fe–B powders with similar particle sizes distribution and without particle surface modification (uncoated).[16]

3.2 Mechanical tests

The values of storage modulus under ambient conditions, observed by DMA were compared to the elastic modulus obtained by the tensile and flexural tests (Fig. 2). In contrast to Deng, S. *et al.*[15] mechanical properties at temperatures higher than ambient are not compared with DMA results observed using two different clamps. It seems that observing the elastic modulus of composites by tensile, flexural and DMA tests at room temperature in the present study provides a better understanding to the increasing trend of elastic components of materials with increasing Nd–Fe–B filler content in the polymer matrix.

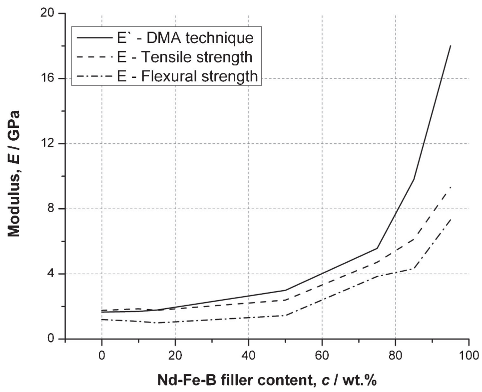

Fig. 2 Comparative view of the changes in the modulus of elasticity at 25°C.

The modulus of elasticity is a very important parameter for analysis of the composite materials behaviour under discontinuous load conditions. The elastic modulus values, obtained by tensile and flexural tests, upswing with an increasing amount of Nd–Fe–B powder from 50 mass% achieve 9.2 and 7.1 GPa, respectively. Within the narrow region and up to 20 mass% content of Nd–Fe–B, where the modulus of elasticity is practically constant according to tensile and flexural tests, dynamic-mechanical analysis could be applied to acquire additional information's related to the mechanical behaviour about transitions in polymer composites.[17]

Modules of elasticity obtained by three presented tests are increased with higher quantities of magnetic filler (Fig. 2). This is crucial in analysis of possible uses of the investigated magnetic composite materials as functional material. This means that materials with higher amounts of Nd–Fe–B filler, subject to equal stress levels (ballast), tolerate 2 to 3.5 times lower deformation.

3.3 Mathematical prediction of Nd–Fe–B/epoxy composite behaviour

The strong influence of relatively small amounts of filler particles on the dynamic mechanical properties of polymers has significantly contributed to increased use of polymer materials in many commercial applications.[18] The incorporation of filler particles is known to increase the stiffness of the material and alter time dependent aspects of material behaviour such as hysteresis and stress relaxation. Even under strains sufficiently large for the structure to have been eliminated, the storage modulus is greater than that of the pure polymer, and greater than the amount which can be predicted due to hydrodynamic interaction of the filler particles.

Ideally, in an attempt to reduce laboratory costs, one would like to make a prediction of a new material's behaviour using numerical simulation procedures, with the primary goal being to accelerate trial and error experimental testing.

Analytical models are easy to apply and require only properties of individual constituents of composite and their fraction. Proposed analytical models are tested versus experimental data as illustrated in following section. Some of the applied models are in good agreement with experimental data, whilst others deviate significantly.

There have been several attempts to derive formulas giving the apparent modulus according to a dispersion of particles in polymer. The earliest of these attempts was by Smallwood using the analogy to Einstain's viscosity equation.[19] Smallwood's estimate is only good at very low filler concentrations. A number of attempts have been made to incorporate interactions between neighbouring particles to allow prediction for higher volume fractions. Most of these models add one or more terms to a polynomial series expansion. One of the most cited model of this class is the Guth–Gold.[20] Later Guth extended the Guth–Gold model to include the impact of particle shape on properties. Guth introduced a shape factor f (ratio of diameter to width of particle) and proposed a new equation.[21] Budiansky developed a model, for the special case of rigid particles in an incompressible matrix[22] while the Ponte Castaneda has proposed a different self-consistent estimate for rigid particles in a neo-Hookean matrix.[23] Later Govindjee and Simo proposed the novel model, for the case of rigid particles in a neo-Hookean matrix.[24] In addition, it is worth to mention the empirical formula suggested by Brinkmann.[25]

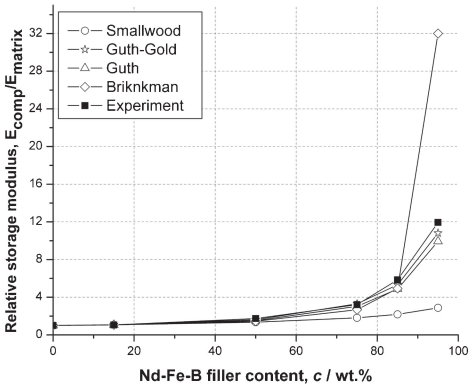

Fig. 3 Models predictions against experimental data.

Major characteristics of all aforementioned theoretical models are: they neglect the impact of filler properties and assume that the medium wets the filler particles, and they do not chemically react with the filler surface. The experimentally obtained values of storage modulus are compared with analytical models discussed above and presented in Fig. 3.

Predictions of models proposed by Budiansky, Ponte Castaneda and Govindjee-Simo give inadequate estimation so they are not included in Fig. 3. From Fig. 3 one may notice that all models included in analysis give very good predictions of storage modulus towards lower particles concentrations (till 50 mass%). This suggests that within low concentration ranges, the interactions between neighbouring particles have a very low intensity. At higher concentrations, the interactions become high intensity which is the main reason for the significant deviation of Smallwood's model from experimental results. Brinkman's model gives good predictions at high concentrations, but at very high concentrations of particles, it extensively overpredicts the storage modulus. The Guth and Guth–Gold models are in very good agreement with experimental results. The explanation for this behaviour lies in the fact that both models take into consideration interactions between neighbouring particles.

In contradiction to the aforementioned explicit models, Mori Tanaka model takes into consideration the impact of the filler properties and particle arrangement on composite properties.

$$E'_{\mathrm{comp}} = E'_{\mathrm{matrix}} \frac{1 + \dfrac{7-5\upsilon_{\mathrm{m}}}{8-10\upsilon_{\mathrm{m}}} \cdot \dfrac{E_{\mathrm{P}}/E'_{\mathrm{matrix}} - 1}{E_{\mathrm{P}}/E'_{\mathrm{matrix}} + \dfrac{7-5\upsilon_{\mathrm{m}}}{8-10\upsilon_{\mathrm{m}}}} \cdot V_{\mathrm{P}}}{1 - \dfrac{E_{\mathrm{P}}/E'_{\mathrm{matrix}} - 1}{E_{\mathrm{P}}/E'_{\mathrm{matrix}} + \dfrac{7-5\upsilon_{\mathrm{m}}}{8-10\upsilon_{\mathrm{m}}}} \cdot \left[1 + \left(\dfrac{1-\phi_{\max}}{\phi_{\max}^2}\right) \cdot V_{\mathrm{P}}\right]} \tag{1}$$

Equation (1) shows that storage modulus of composites depends on components storage modulus (E'_{matrix}, E'_{P}), Poisson's ratio of polymer matrix (υ_{m}), volume fraction of filler (V_{P}) and maximum packing factor ($\phi_{\max}$).

Storage moduli of components have a constant value for specific temperature as well as Poisson's ratio. Therefore, the only variable is maximum packing factor. In original MT model developed for one-dimensional spherical particles, maximal packing factor is assumed to be constant value and independent of particle size and distribution.[26] Later, Kwon *et al.* extended MT model to multidimensional spherical particles.[27] This model considers that maximum

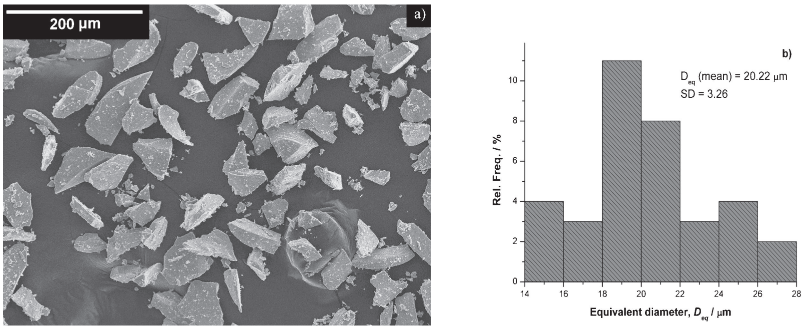

Fig. 4 (a) SEM micrograph and (b) equivalent diameters distribution of Nd–Fe–B particles.

packing factor is dependant on particle size and particle distribution.

In order to apply Kwon *et al.* model,[27] irregular plate like particles are approximated with multi-dimensional spherical particles using equivalent diameters (D_{eq}) defined as follows:

$$V_p = A_p \cdot t = \frac{1}{6} \cdot D_{eq}^3 \cdot \pi \tag{2}$$

Surface area (A_p) and thickness (t) of irregular plate-like particles are determined from SEM micrographs by image analysis using Image Pro Plus software.[28] The data obtained from image analysis are based on the shape and size of elements observed in the pictures. Application of the method is described by Veljovic *et al.*[29] and Bajat *et al.*[30]

Volume (V_p) and equivalent diameter (D_{eq}) are calculated applying eq. (2). The median equivalent diameters of particles are estimated from equivalent diameters distribution, as shown in Fig. 4(b).

The results obtained by experiment and mathematical model developed by Kwon *et al.* are presented in Fig. 5 shows that values predicted by Kwon *et al.* model for filler content less than 50 mass% are tracking the trend of experimental curve. Therefore, the constant value of packing factor does not have a huge impact on the estimated values of the modulus. As the content of filler rises, the deviation between the trends becomes more obvious. For the Nd–Fe–B content higher than 85 mass% model shows significant deviation, which is probably a consequence of a constant maximal packing factor value of 0.633.

According to aforementioned, it seems that maximum packing factor depends on filler content. In order to prove this assumption maximum packing factor is evaluated for different content of Nd–Fe–B filler by minimizing deviation between model and experimental values [eq. (3)].

$$\min \Phi = \sum \frac{(E'^{exp}_{comp} - E'^{model}_{comp})^2}{E'^{exp}_{comp}} \tag{3}$$

Evaluated modulus values (Fig. 5) for optimized maximal packing factors (Table 1) are in excellent match with experimental results. Obtained values of packing factor are within realistic range from 0 to 1.

Analyzing these results, one can conclude that there is a strong relationship between maximal packing factor and structural properties of composites. This relationship may be explained by introducing the packing density into the analysis. Optimal process parameters, particle distribution,

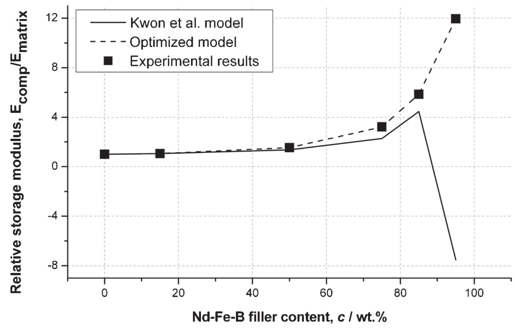

Fig. 5 Storage modulus obtained by: experiment, Kwon *et al.* model and optimized MT model.

Table 1 Maximal packing factor for different content of Nd–Fe–B filler.

Nd–Fe–B, c/mass%	Maximal packing factor, Φ_{max}	
	Optimized MT model	Kwon *et al.* model
15	0.2997	0.6332
50	0.3235	
75	0.4539	
85	0.5746	
95	0.8489	

particle shape and size, packing density, and good adhesion between Nd–Fe–B and a polymer matrix, are all essential for microstructure, stiffness and magnetic properties of the final composite material.[31] The packing density can be increased by mixing powder fractions of different particle size and size distribution. The optimized powder mixture has small particles filling the inter-particle volume of packing of larger particles. Generally speaking, the plate-like particles would result in higher packing density under the optimal compression conditions.[32,33] SEM micrographs of composites fracture surface in Fig. 6 clearly illustrate a packing density for different Nd–Fe–B content.

Although Nd–Fe–B particles are of variable size and shape, they seem to be attached rather well to the matrix. According to SEM micrographs [Figs. 6(a)–6(c)], it is obvious that packing density increases with rising Nd–Fe–B filler content. For highly filler bonded magnets pressure has direct influence on structure and magnetic properties. According to Zhang *et al.*,[32] pressure higher than 620 MPa could cause structural damages of composite resulting in

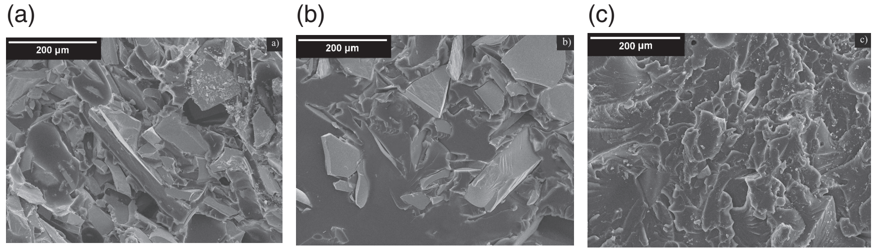

Fig. 6 SEM micrographs of composites with (a) 95 mass%, (b) 50 mass% and (c) 20 mass% of Nd–Fe–B filler (Nd–Fe–B particles are shown as light grey and the epoxy matrix is shown as dark grey colour).

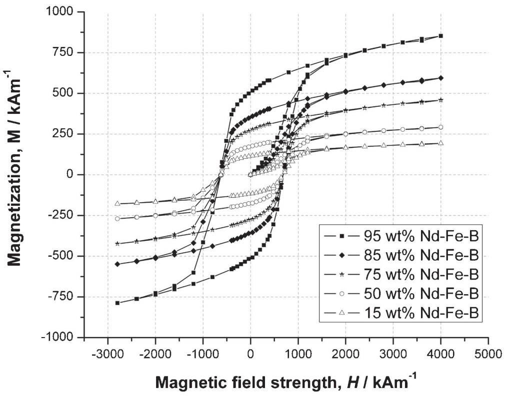

Fig. 7 Hysteresis loops of magnetic composites.

downswing of mechanical (magnetic) properties. Conversely, pressure has a slight or no impact on pure epoxy sample and composites with low filler content. In order to determine comparative experimental results, composites with a constant volume, but different particle to epoxy matrix ratio are prepared at constant pressure.

According to the results obtained, packing density and maximal packing factor rise with increasing content of particles. This infers that a strong relationship between these two packing factors exist for composites with irregular plate-like particles.

3.4 Magnetic properties

Magnetic properties of composite materials (bonded magnets) are affected by the magnetic properties of the magnetic powder and weight (volume) ratio of the powder. It is known that bonded magnets have inferior magnetic characteristics compared to magnetic material obtained by convectional methods (sintering for example), because in the bonded technology can not be achieved the maximal density of magnetic powder.[32] One of the most important characteristics of the used type of Nd–Fe–B rare-earth magnetic material is the high remanence and coercivity values which have a direct influence on high values of maximal energy product.[34] The results of magnetic measurements i.e. complete hysteresis loops for bonded Nd–Fe–B/epoxy type magnets with different contents of functional magnetic particles are presented in Fig. 7. It is obvious that the largest hysteresis loop correspond to the magnetic composite with the highest amount of magnetic component.

Based on these results, corresponding B-H diagrams are constructed, and the changes of remanence (B_r), coercivity (H_{cb}) and maximal energy product (BH_{max}) with an increasing content of Nd–Fe–B in the epoxy matrix are taken and presented in Table 2.

Table 2 Magnetic and dynamic mechanical properties of composites.

Nd–Fe–B, c/mass%	B_r/T	H_{cb}/kA·m^{-1}	$(BH)_{max}$/kJ·m^{-3}
15	0.14	111.4	3.2
50	0.23	159.2	8.0
75	0.35	238.7	19.1
85	0.45	302.4	34.2
95	0.64	382.0	62.9

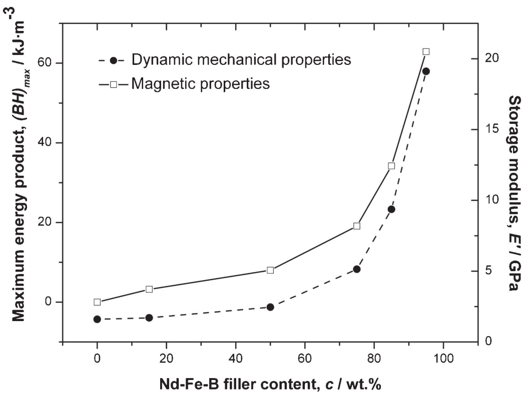

Fig. 8 The magnetic and dynamic mechanical properties of composites.

The presented results show an increasing trend for three magnetic parameters with increasing amounts of Nd–Fe–B particles in the epoxy matrix. For example, the maximal energy product for composite with 95 mass% Nd–Fe–B is around 8 MGOe, which is two times higher than for the composite with the 85 mass% Nd–Fe–B case. For composites with Nd–Fe–B content higher than 75 mass%, $(BH)_{max}$ rapidly increases i.e. for the highly filled composites even a small addition of magnetic medium can have a strong influence on the magnetic properties of bonded magnets. Also, the maximum energy product $(BH)_{max}$ of Nd–Fe–B bonded magnets can be simulated using a mathematical model. Moreover, choosing appropriate parameters for the magnetic texture and the magnetic coupling between micrograins can increase the value of $(BH)_{max}$.[35,36]

The comparison of magnetic and dynamic mechanical properties is illustrated in Fig. 8. Due to fact that magnetic and dynamic mechanical properties show the same trend with filler content enhancement, it can be concluded that there is a strong relationship between these properties.

4. Conclusion

The results of this study show that addition of plate-like Nd–Fe–B particles to the polymer affects the rheological properties the polymer matrix via internal structural changes, and subsequently impacts the dynamic mechanical strength of bonded magnets.

DMA data show that the value of storage modulus amplifies in glassy, as well as in rubbery state, as the concentration of filler in composite rises. The tensile and flexural tests at ambient temperature show enhancement of modulus of elasticity with quantity of magnetic filler, which is a crucial parameter for analyzing of composite materials behaviour. Information extracted from tensile and flexural tests are consistent with results evaluated by DMA. Introduction of equivalent diameters distribution and consequently set of maximal packing factor values have a direct impact on the results in wide range of Nd–Fe–B filler content. After optimization, the widely used Mori Tanaka mathematical model show excellent agreement with experimental results and could be used as a potential model for further predictions of dynamic mechanical behaviour.

As expected, magnetic properties are drastically improved with a higher content of Nd–Fe–B magnetic particles, especially for highly filled composites. These results provide information about the Nd–Fe–B/epoxy composites which could be of importance in cases where the relatively brittle metallic permanent magnets are not useable.

Considering the increasing interest in polymer composites and advanced analytical tools, the present study provides a useful basis for future experiments and theory development for multifunctional components and commercially important polymer bonded magnets.

Acknowledgement

The authors are grateful to Ms Sabla Alnouri from Texas A&M University at Qatar for the assistance during the research activities. This work is supported by Ministry of Education and Science, Republic of Serbia, under projects TR 34011 and III 45019.

REFERENCES

1) K. Hono and D. H. Ping: Mater. Sci. Eng. A **304–306** (2001) 81–87.
2) Y. Matsuura: J. Magn. Magn. Mater. **303** (2006) 344–347.
3) D. N. Brown, Z. Chen, P. Guschl and P. Campbell: J. Magn. Magn. Mater. **303** (2006) e371–e374.
4) J. Li, Y. Liu, S. J. Gao, M. Li, Y. Q. Wang and M. J. Tu: J. Magn. Magn. Mater. **299** (2006) 195–204.
5) T. S. Chin: J. Magn. Magn. Mater. **209** (2000) 75–79.
6) O. Gutfleisch, M. A. Willard, E. Brück, C. H. Chen, S. G. Sankar and J. P. Liu: Adv. Mater. **23** (2011) 821–842.
7) L. A. Dobrzanski, M. Drak and B. Ziebowicz: J. Mater. Process. Technol. **191** (2007) 352–355.
8) M. G. Garrell, B. M. Ma, A. J. Shih, E. Lara-Curzio and R. O. Scattergood: Mater. Sci. Eng. A **359** (2003) 375–383.
9) K. P. Menard: *Dynamic Mechanical Analysis: A Practical Introduction*, (CRC Press LLC, Florida, 1999).
10) J. D. Ferry: *Viscoelastic Properties of Polymers* (3rd edition), (John Wiley & Sons, Inc., New York, 1980).
11) A. S. Grujić, N. L. Lazić, N. M. Talijan, V. Spasojević, J. T. Stajić-Trošić, V. R. Ćosović and R. Aleksić: Acta Physiol. Pol. A **117** (2010) 859–863.
12) A. Grujić, V. Ćosović, J. Stajić-Trošić, N. Talijan, V. Spasojević, N. Lazić and R. Aleksić: Proc. 21st Workshop on Rare-Earth Permanent Magnets and their Applications, ed. by Spomenka Kobe and Paul McGuiness, (Jožef Stefan Institute, Ljubljana, 2010) pp. 213–216.
13) A. R. Payne: *Dynamic Properties of Filler-Loaded Rubbers*, *Reinforcement of Elastomers*, Kraus G., (Interscience Publishers, a division of John Wiley & Sons, USA, 1965) pp. 69–123.
14) M. J. Wang: Rubber Chem. Technol. **72** (1999) 430–448.
15) S. Deng, M. Hou and L. Ye: Polym. Test. **26** (2007) 803–813.
16) J. U. Otaigbe, H. S. Kim and J. Xiao: Polym. Compos. **20** (1999) 697–704.
17) T. Maity, B. C. Samanta, S. Dalai and A. K. Banthia: Mater. Sci. Eng. A **464** (2007) 38–46.
18) J. S. Bergstrom and M. C. Boyce: Rubber Chem. Technol. **72** (1999) 633–656.
19) J. P. Donnet: Rubber Chem. Technol. **71** (1998) 323–341.
20) E. Guth and O. Gold: Phys. Rev. **53** (1938) 322.
21) E. Guth: J. Appl. Phys. **16** (1945) 20–25.
22) B. Budiansky: J. Mech. Phys. Solids **13** (1965) 223–227.
23) P. Ponte Castaneda: Proc. R. Soc. London Ser. A **422** (1989) 147–171.
24) S. Govindjee and J. C. Simo: J. Mech. Phys. Solids **39** (1991) 87–112.
25) H. C. Brinkman: J. Chem. Phys. **20** (1952) 571.
26) T. Mori and K. Tanaka: Acta Metal. **21** (1973) 571–574.
27) S. C. Kwon, T. Adachi, W. Araki and A. Yamaji: Acta Mater. **54** (2006) 3369–3374.
28) http://www.mediacy.com
29) Dj. Veljovic, R. Jancic-Hajneman, I. Balac, B. Jokic, S. Putic, R. Petrovic and Dj. Janackovic: Ceram. Int. **37** (2011) 471–479.
30) J. B. Bajat, I. Milosev, Z. Jovanovic, R. M. Jancic-Heinemann, M. Dimitrijevic and V. B. Miskovic-Stankovic: Corros. Sci. **52** (2010) 1060–1069.
31) P. C. Guschl, H. S. Kim and J. U. Otaigbe: J. Appl. Polym. Sci. **83** (2002) 1091–1102.
32) X. H. Zhang, W. H. Xiong, Y. F. Li and N. Song: Mater. Design **30** (2009) 1386–1390.
33) D. Rodrigues, G. V. Concilio and F. G. Landgraf: Proc. 14th International Workshop Rare-Earth Magnets and Their Applications, (World Scientific, Sao Paulo, Brazil, 1996) Vol. 1, pp. 580–589.
34) O. Gutfleisch: J. Phys. D Appl. Phys. **33** (2000) R157–R172.
35) N. V. Vuong, N. V. Khanh and D. M. Thuy: Phys. B **327** (2003) 349–351.
36) J. Xiao, J. U. Otaigbe and D. C. Jiles: J. Magn. Magn. Mater. **218** (2000) 60–66.